Generation and Acceleration of High-Density Helicon Plasma Using Permanent Magnets for the Completely Electrodeless Propulsion System*)

Shuhei OTSUKA, Toshiki NAKAGAWA, Hiroki ISHII, Naoto TESHIGAHARA, Hiroaki FUJITSUKA, Shimpei WASEDA, Takamichi ISHII, Daisuke KUWAHARA and Shunjiro SHINOHARA

Tokyo University of Agriculture and Technology, 2-24-16 Naka-Cho, Koganei, Tokyo 184-8588, Japan

(Received 18 November 2013 / Accepted 14 March 2014)

In our proposed method of the completely electrodeless electric propulsion system, a high-density ($\sim 10^{13}\,\mathrm{cm}^{-3}$) helicon plasma is accelerated by the Lorentz force, i.e., the product of the azimuthal current j_θ and the radial component of magnetic field B_r. In order to promote the plasma acceleration scheme, we used permanent magnets (PMs) designed to increase B_r in comparison to the present electromagnets (EMs). As an initial try of the plasma acceleration by our system, electron density n_e and ion velocity v_i of generated plasma using PMs' magnetic field were measured, and we have obtained the maximum value of $n_\mathrm{e} = 2.5 \times 10^{12}\,\mathrm{cm}^{-3}$ and $v_\mathrm{i} = 2.2\,\mathrm{km/s}$. In addition, we have also introduced a combined, flexible operation of using PMs and EMs leading to better plasma performance.

Keywords: helicon plasma, electrodeless electric propulsion, permanent magnet, magnetic nozzle

DOI: 10.1585/pfr.9.3406047

1. Introduction

Electric propulsion system is expected to be a useful method for long-term space missions, for example, Jupiter or Saturn exploration because its specific impulse (exhaust velocity divided by gravity) is larger than chemical one. However, most of the systems have electrodes for plasma generation and acceleration, thus causing a significant decrease of the lifetime due to the direct contact between the plasma and electrodes. This problem can be resolved by using completely electrodeless electric propulsion system which we propose as a Helicon Electrodeless Advanced Thruster: HEAT project [1]. This system in our team consists of two electromagnetic acceleration methods: acceleration by Rotating Magnetic Field (RMF) coils [1, 2] and a half cycle acceleration by $m = 0$ mode coil [1]. These acts on a high-density ($\sim 10^{13}\,\mathrm{cm}^{-3}$) helicon plasma [3–5], and the plasma is accelerated by the Lorentz force generated by the azimuthal current j_θ induced in the plasma and the radial component of the magnetic field B_r.

We were using electromagnets (EMs) to produce external magnetic field B in our previous study, because magnetic configuration can be changed easily. However, B_r required for plasma acceleration is insufficient (few tens of Gauss) when forming a divergent magnetic field by the EMs. In this study, we have tried to solve this problem by introducing permanent magnets (PMs) [6] to increase B_r. Advantages of PMs are the followings. (1) PMs' magnetic field (surface magnetic field is $\sim 1.5\,\mathrm{kG}$ in our case) is very strong in spite of more compact size than EMs. (2) It is possible to generate the magnetic field in a localized region, because PMs' magnetic field becomes weaker very rapidly away from PMs unlike EMs. (3) Since PMs do not consume electric power, they can be useful sources to produce the magnetic field in space with a limited electric power.

We have designed an original, divergent magnetic field shape by PMs, which is suitable for plasma acceleration, and conducted plasma generation experiments under this field. In this paper, we report initial measurement results of electron density n_e and ion velocity v_i of target plasmas (without RMF coils and $m = 0$ mode coils). Furthermore, as a next stage, we have tried high-density plasma generation by the magnetic field configuration in combination with PMs and EMs.

2. Concept of the Plasma Acceleration

As was mentioned for a longer lifetime operation, plasma is not contact with the electrodes directly in our proposed plasma acceleration method. Here, our concept can be executed as follows. First, plasma is generated in a quartz tube by a radio frequency (RF) power via an RF antenna. Next, j_θ is induced in the plasma using an acceleration antenna, such as RMF coils. These antennas are installed outside of the tube; therefore, they will not be

author's e-mail: 50013643016@st.tuat.ac.jp

*) This article is based on the presentation at the 23rd International Toki Conference (ITC23).

deteriorated by the plasma. Applying B_r by the external magnetic field sources, the Lorentz force in the axial direction is produced by $j_\theta \times B_r$ (see Fig. 1), and plasma is accelerated by this force. As a reactive force of this, thrust force is obtained.

Here, the thrust of ions is proportional to the product of n_e and the square of v_i, and thus, they should be higher to have the larger thrust.

3. Experimental Device

3.1 Large Mirror Device

Figure 2 shows a schematic diagram of the Large Mirror Device (LMD) [7] (1,700 mm in axial length and 445 mm in inner diameter). The quartz tube, 1,000 mm in axial length, had a tapered shape (100 ~ 170 mm in inner diameter) to prevent a wall loss of divergent plasma. Background pressure in LMD was a few times of 10^{-4} Pa. Ar gas was used as a propellant, and a typical discharge pressure range was 0.5 ~ 1 Pa. RF input power was ~ 3 kW with the excitation frequency of 7 MHz. The external B can be generated by EMs and PMs.

3.2 Permanent magnets

A structure called "magnet holder" for fixing the PMs around the quartz tube was manufactured. The advantage of our holder is that the magnetic field strength can be changed by selecting a number of PM sheets (between 1 and 3) in each position. There were 100 locations where PM sheets are fixed, and each sheet size had $50 \times 25 \times 5\,\mathrm{mm}^3$. Here, Neodymium (NdFeB) magnets were used, and their grade was N35 made by NeoMag Co. Ltd.: 33 ~ 36 MGOe in maximum energy product and ~ 1,590 G in surface magnetic flux density with the magnetization direction toward the center of a quartz tube. PMs' magnetic field strength and their field lines in the case of 300 PM sheets are shown in Fig. 3. It can be seen that PMs form a strong and divergent magnetic field (the magnetic nozzle) locally. Figure 4 shows axial profiles of B_r of the PMs and EMs on a line of r = 50 mm in the plasma acceleration area. By comparing the maximum value, B_r of PMs is about four times larger than that of EMs. Positions of the EMs are provided for forming the divergent magnetic field near the tapered tube area, and three leftmost EMs shown

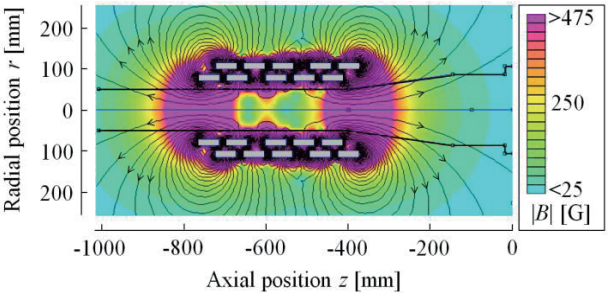

Fig. 3 Magnetic field strength and its field lines of PMs.

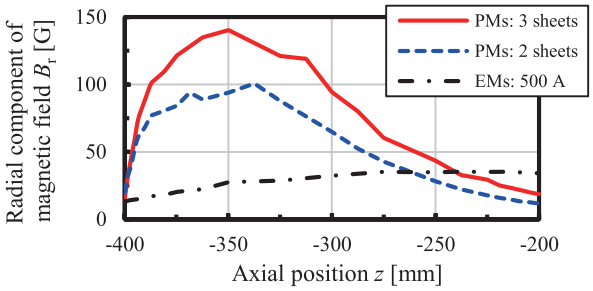

Fig. 4 Axial profiles of magnetic field B_r of PMs and EMs on a line of r = 50 mm in the area of plasma acceleration.

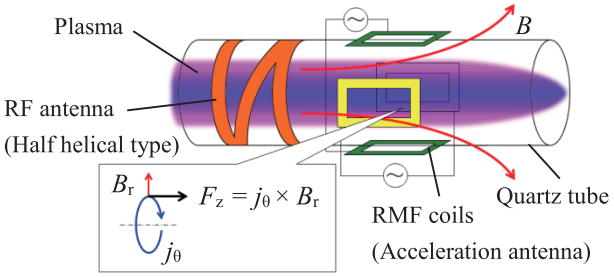

Fig. 1 Principle of electrodeless plasma acceleration method (RMF case).

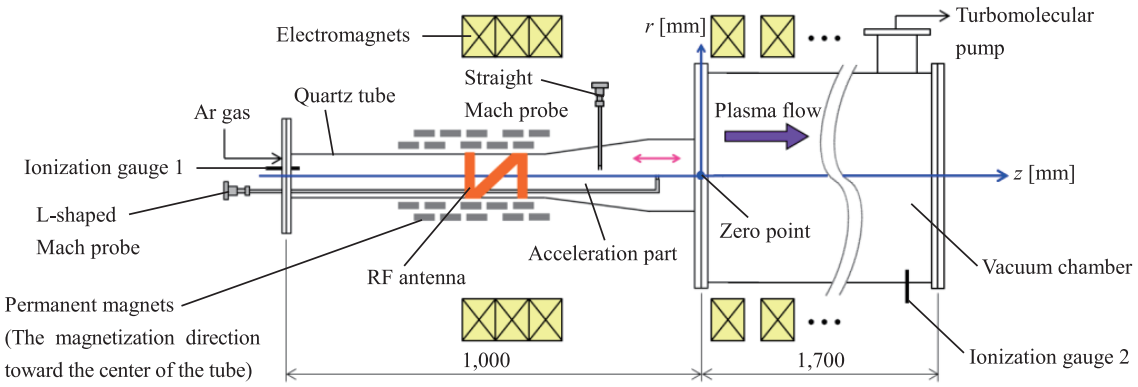

Fig. 2 Schematic diagram of LMD.

in Fig. 2 are used in this calculation. Here, Figs. 3 and 4 were calculated using the finite element method, and there is only a ~1% difference compared to value measured by Gaussmeter, Lake Shore 410 (minimum resolution: 0.1 G).

4. Experimental Results

In order to verify the effects of the PMs' magnetic field, two types of experiments were carried out: (1) axial distributions of n_e and v_i with and without EMs, in the presence of PMs. (2) axial distributions of n_e and v_i changing the number of sheets (2 or 3 sheets each position of magnet holder) using only PMs. Experimental conditions are shown in Table 1 (measurement positions of the gas pressure are shown in Fig. 2). In the measurements, a L-shaped Mach probe was used to scan the axial position. Here, for flow measurement by this probe, we used the unmagnetized model (model constant $\kappa = 1.26$) [8, 9].

4.1 Experiment (1)

Figure 5 (a) shows that n_e using PMs only was higher than the case of EMs only and also no magnetic field case in most positions. Comparing the maximum value, n_e using PMs was about 1.8 times higher than other two cases. In Fig. 5 (b), v_i in the case of PMs was also higher than using EMs and no magnetic field in most positions. The maximum value of v_i using PMs was about 2.2 (3.4) times higher than that of EMs (no magnetic field). Thus, PMs only had an effect of improving n_e and v_i, and it can contribute to increases of the thrust.

4.2 Experiment (2)

Here, the number of PMs was increased from 2 to 3 sheets, and the magnetic field also became stronger by about 1.5 times, as shown in Fig. 4. From Fig. 6 (a), n_e did not change regardless of the magnet number except $z = -500$ mm position.

Figure 6 (b) shows axial profiles of v_i, changing the number of PM sheets. When the number of PM sheets was increased from 2 to 3, v_i also increased in region of $z = -400 \sim -100$ mm and its maximum value was 2.2 km/s.

Table 1 Experimental conditions.

Parameters		Experiment (1)	Experiment (2)
Gas flow rate		25 sccm	50 sccm
Gas pressure	Gauge 1	0.62 Pa	0.90 Pa
	Gauge 2	0.094 Pa	0.16 Pa
External B		· w/o B · EMs (500 A) · PMs (2 sheets)	PMs · 2 sheets each · 3 sheets each
RF power		2 kW	
Measurement position	r	0 mm	
	z	-700 ~ -100 mm	

According to the measurement by a high resolution monochromator and Laser Induced Fluorescence (LIF) [10] method in almost same condition, the maximum value of v_i in this region were 2.9 km/s and 2.6 km/s, respectively. These three measurement methods have shown fairly good agreements, although Mach probe data had slightly smaller values. Here, the monochromator was Czerny-Turner type MC-150 (wavelength range: 190 ~ 600 nm, grating: 2,400 lines/mm and resolution: 0.006 nm) made by Ritsu

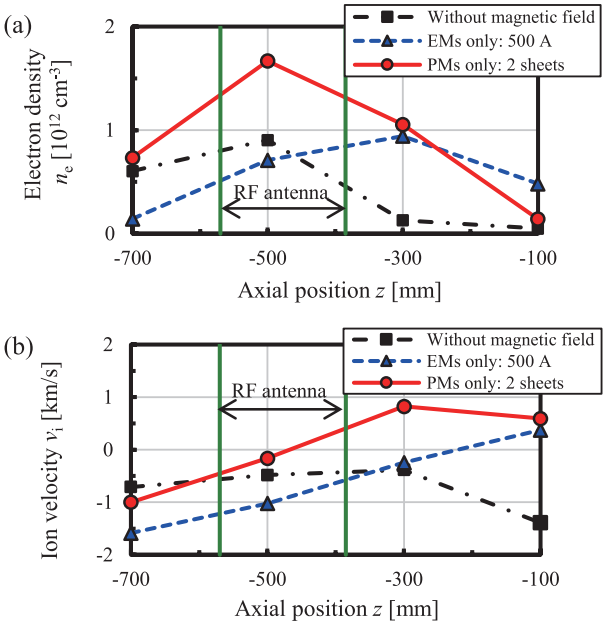

Fig. 5 Axial distributions of (a) n_e and (b) v_i, changing the magnetic field configuration: no magnetic field, EMs and PMs.

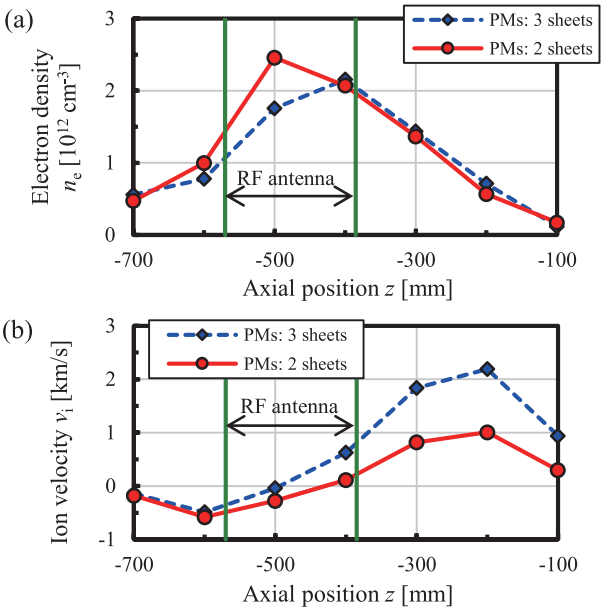

Fig. 6 Axial distributions of (a) n_e and (b) v_i, changing the number of PM sheets (2 or 3 sheets in each position of magnet holder).

Ouyou Kougaku. In the LIF system, the tunable diode laser was TA100 made by Toptica Co. (oscillating frequency: 663.5 ~ 669.3 nm, wavelength width: 1 MHz and maximum of output power: 500 mW).

Magnetic field gradient in addition to plasma pressure gradient, is considered to change the ion velocity. If the latter can be neglected, the force $\boldsymbol{F}$ shown below can act on plasma in the axial direction,

$$\boldsymbol{F} = -\mu \nabla B, \tag{1}$$

where μ is the magnetic moment of the gyrating particle. From Fig. 3, the negative magnetic field gradient, whose term is a few times larger than the pressure gradient one, exists in the region of $z > -400$ mm, and v_i increased monotonically. However, v_i decreased in the region of $z = -200 \sim -100$ mm partly due to effects of the smaller decreasing magnetic field gradient and the increased plasma loss since the divergent magnetic field lines hit an inner quartz wall surface.

5. Advanced Study

To reduce the wall losses of the plasma mentioned, we are now studying a plasma generation and acceleration using the magnetic field in combination with PMs and EMs. Although EMs are not suitable to make large B_r, they can modify the magnetic field shape and strength by changing their axial position and the current. As the first step, we show one calculation result with the combined magnetic field configuration, as shown in Fig. 7. Large B_r by PMs is not changed, by generating a nearly uniform field by EMs, and consequently the magnetic field lines do not hit the wall. The maximum value of combined magnetic field strength is 1.4 kG on position of $z = -393$ mm and $r = 0$ mm. Figure 8 shows experimental results of n_e by comparing the cases of the combination of magnetic fields, PMs and EMs, and the field by PMs only. Here, gas flow rate was 50 sccm, RF power was 3 kW, and the measurement positions were $z = -275$ mm, and $r = 0 \sim 60$ mm. In this axial position, wall losses of the plasma were considered to be greater with PMs only (see Fig. 3).

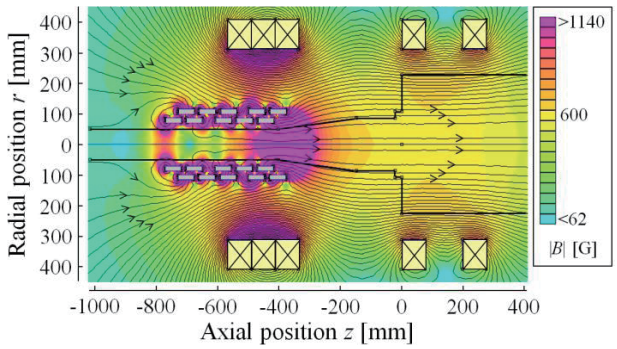

Fig. 7 Magnetic field strength and its field lines in combination with PMs and EMs.

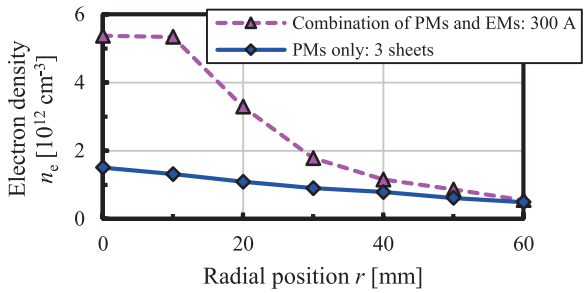

Fig. 8 Radial distributions of n_e using both PMs and EMs, or using PMs only.

By adding EMs' magnetic field to PMs', n_e increased significantly. The maximum value of n_e in the combined magnetic field case is 5.4×10^{12} cm^{-3} which is about 3.6 times higher compared to n_e in the case of only PMs (3 sheets case), showing a possibility that wall losses of the plasma were reduced and/or the total plasma confinement was enhanced because of the stronger axial magnetic field.

6. Conclusion

To realize an electrodeless electric propulsion system proposed, the magnetic field configuration by PMs, suitable for plasma generation and acceleration, was designed. By using PMs, we have investigated axial distributions of n_e and v_i, important parameters of the plasma thrust, and succeeded in increasing them than EMs only by a few times: The maximum values attained were $n_e = 2.5 \times 10^{12}$ cm^{-3} and $v_i = 2.2$ km/s. We will make a comparison study as to various plasma parameters, especially plasma flow, by using the method by the high-resolution monochromator and LIF method in addition to Mach probes.

Furthermore, as an advanced study, the combined operation using PMs and EMs has been done. The maximum value was $n_e = 5.4 \times 10^{12}$ cm^{-3}, which was about 3.6 times compared to the n_e in the case of PMs only, showing a reduction of the wall losses of plasmas.

For the plasma generation in order to get target plasmas for acceleration, it is necessary to optimize this combined magnetic field configuration to reduce the wall losses of plasmas and the increase n_e under the various experimental conditions. From these findings, we will apply the electromagnetic acceleration by RMF or $m = 0$ coils, using the optimized target plasmas obtained.

Acknowledgements

We appreciate useful discussions made by HEAT project members. This study has been supported by Grant–in–Aid for Scientific Research (S: 21226019) from the Japan Society for the Promotion of Science.

[1] S. Shinohara *et al.*, Fusion Sci. Technol. **63**, 164 (2013).
[2] I.R. Jones, Phys. Plasmas **6**, 1950 (1999).
[3] R.W. Boswell, Phys. Lett. **33A**, 457 (1970).

[4] S. Shinohara, Jpn. J. Appl. Phys. **36**, 4695 (1997).
[5] R.W. Boswell and F.F. Chen, IEEE Trans. Plasma Sci. **25**, 1229 (1997).
[6] K. Takahashi *et al*., Phys. D: Appl. Phys. **44**, 01524 (2011).
[7] S. Shinohara *et al*., Jpn. J. Appl. Phys. **35**, 4503 (1996).
[8] M. Hudis and L.M. Lidsky, J. Appl. Phys. **41**, 5011 (1970).
[9] K.S. Chung *et al*., Phys. Fluids **B1**, 2229 (1989).
[10] R.F. Boivin *et al*., Rev. Sci. Instrum. **74**, 4352 (2003).